HHS Public Access

Author manuscript

Cell. Author manuscript; available in PMC 2016 January 15.

Published in final edited form as:

Cell. 2015 January 15; 160(0): 88–104. doi:10.1016/j.cell.2014.12.022.

Leptin and insulin act on POMC neurons to promote the browning of white fat

Garron Dodd[1], **Stephanie Descherf**[1], **Kim Loh**[1], **Stephanie E. Simonds**[2], **Florian Wiede**[1], **Eglantine Balland**[2], **Troy L. Merry**[1], **Heike Münzberg**[3], **Zhong-Yin Zhang**[4], **Barbara B. Kahn**[5], **Benjamin G. Neel**[6], **Kendra K. Bence**[7], **Zane B. Andrews**[2], **Michael A. Cowley**[2], and **Tony Tiganis**[1,*]

[1]Department of Biochemistry and Molecular Biology, Monash University, Victoria 3800, Australia

[2]Department of Physiology, Monash University, Victoria 3800, Australia

[3]Pennington Biomedical Research Center, LSU Systems, Baton Rouge, LA 70808

[4]Department of Biochemistry and Molecular Biology, Indiana University School of Medicine, Indianapolis, IN, 46202-5126

[5]Division of Endocrinology, Diabetes and Metabolism, Department of Medicine, Beth Israel Deaconess Medical Center and Harvard Medical School, Boston, MA 02215

[6]Campbell Family Cancer Research Institute, Ontario Cancer Institute, Princess Margaret Hospital and Department of Medical Biophysics, University of Toronto, Toronto, Ontario, Canada

[7]Department of Animal Biology, School of Veterinary Medicine, University of Pennsylvania, Philadelphia, PA 19104

SUMMARY

The primary task of white adipose tissue (WAT) is the storage of lipids. However, 'beige' adipocytes also exist in WAT. Beige adipocytes burn fat and dissipate the energy as heat, but their abundance is diminished in obesity. Stimulating beige adipocyte development, or WAT browning, increases energy expenditure and holds potential for combating metabolic disease and obesity. Here we report that insulin and leptin act together on hypothalamic neurons to promote WAT browning and weight loss. Deletion of the phosphatases PTP1B and TCPTP enhanced insulin and leptin signaling in proopiomelanocortin neurons and prevented diet-induced obesity by increasing WAT browning and energy expenditure. The co-infusion of insulin plus leptin into the CNS or the activation of proopiomelanocortin neurons also increased WAT browning and decreased adiposity. Our findings identify a homeostatic mechanism for coordinating the status of energy stores, as relayed by insulin and leptin, with the central control of WAT browning.

INTRODUCTION

There are two types of adipose tissue in humans, WAT and brown adipose tissue (BAT). WAT can store vast amounts of energy as triglycerides (TAGs) for utilisation during periods

*Correspondence: Tony.Tiganis@monash.edu.

of fasting or starvation. In contrast, BAT dissipates the chemical energy stored in TAGs as heat to preserve core temperature during hypothermia and to counteract obesity (Rosen and Spiegelman, 2014). Brown adipocytes contain a high density of mitochondria with high amounts of uncoupling protein-1 (UCP-1) allowing for the uncoupling of fatty acid oxidation from ATP production to generate heat (Rosen and Spiegelman, 2014). Although BAT was initially considered to be present only in infants, it is now established that substantial depots of UCP-1 expressing brown-like fat can be detected in the supraspinal, supraclavicular, pericardial and neck regions of adult humans (Cypess et al., 2009; van Marken Lichtenbelt et al., 2009; Virtanen et al., 2009). These brown-like fat depots can be induced in response to cold, but their abundance is diminished in older and obese subjects (Lee et al., 2014; Ouellet et al., 2011).

Brown-like fat is also found in rodents and is composed of beige adipocytes interspersed among white adipocytes (Rosen and Spiegelman, 2014). Under basal conditions beige adipocytes express little to no UCP-1, but UCP-1 induction in response to cold promotes thermogenesis and energy expenditure (Rosen and Spiegelman, 2014). Interestingly, the interscapular BAT in human infants is similar to classical brown fat in rodents (Lidell et al., 2013) whereas, the brown-like fat in adult humans has a molecular signature reminiscent of rodent beige fat (Lidell et al., 2013; Wu et al., 2012). Increasing WAT browning in rodents increases energy expenditure and suppresses diet-induced obesity and glucose intolerance (Seale et al., 2011). On the other hand, preventing WAT browning by deleting *Prdm16*, a transcriptional cofactor that increases UCP-1 expression, promotes obesity and severe insulin resistance (Cohen et al., 2014; Seale et al., 2011). Understanding the molecular processes governing WAT browning is highly significant, as this may identify novel approaches for increasing energy expenditure and combating obesity and the metabolic syndrome. Efforts to date have focussed primarily on the role of factors that act directly on beige pre-adipocytes, such as the irisin and FGF21 (Bostrom et al., 2012; Lee et al., 2014). However, there is mounting evidence that CNS control of WAT browning is also important (Plum et al., 2007; Ruan et al., 2014; Williams et al., 2014).

Leptin is produced by adipocytes and is critical for energy homeostasis and body weight control. Leptin receptors (LEPRs) are expressed in distinct regions of the brain, including the arcuate nucleus (ARC) of the hypothalamus (Myers et al., 2008). The ARC contains at two opposing neuronal populations: the appetite-suppressing proopiomelanocortin (POMC) and the orexigenic neuropeptide Y (NPY) and agouti-related peptide (AgRP)-neuropeptide expressing neurons (Cowley et al., 2001; Elias et al., 1999). Leptin acts on POMC and NPY/AgRP neurons to suppress food intake and promote energy expenditure (Myers et al., 2008). One mechanism by which leptin increases energy expenditure is through the promotion of BAT thermogenesis. Leptin action in the hypothalamus increases sympathetic nerve activity (SNA) to BAT, increasing both UCP-1 expression and BAT activity (Commins et al., 2000; Morrison et al., 2014). Leptin signals via LEPR to activate Janus-activated kinase (JAK)-2, which promotes signaling via effector cascades, including the phosphatidyinositol 3-kinase (PI3K)/AKT and signal transducer and activator of transcription (STAT)-3 pathways, to increase *Pomc* expression and inhibit *Agrp* expression (Myers et al., 2008). The principal role of the melanocortin system in body weight control is underscored by the marked obesity

in humans and rodents with null mutations in the leptin, LEPR or POMC genes (Coll et al., 2004).

Another peripheral factor affecting the melanocortin system is insulin (Varela and Horvath, 2012). Insulin is released from pancreatic β cells following a rise in blood glucose and acts via the insulin receptor (IR) tyrosine kinase and the PI3K/AKT pathway in liver, muscle and fat to lower blood glucose levels (Saltiel and Kahn, 2001). Insulin also acts in the ARC on POMC and AgRP/NPY neurons to regulate whole-body glucose metabolism and elicit anorectic responses (Benoit et al., 2002; Bruning et al., 2000; Konner et al., 2007). One prevailing view is that different POMC neurons exist and that leptin and insulin may act on distinct POMC neuronal subsets (Hill et al., 2010; Sohn et al., 2011; Williams et al., 2010).

The protein tyrosine phosphatases PTP1B (*PTPN1*) and TCPTP (*PTPN2*) regulate body weight and glucose homeostasis (Tiganis, 2013). PTP1B dephosphorylates JAK2 to suppress leptin signaling in hypothalamic neurons, including POMC neurons (Banno et al., 2010; Bence et al., 2006; Tiganis, 2013), whereas TCPTP dephosphorylates STAT3 in the hypothalamus (Loh et al., 2011). We have taken advantage of mice lacking PTP1B, TCPTP or both phosphatases in POMC neurons to demonstrate that PTP1B and TCPTP selectively regulate leptin and insulin signaling to affect body weight, energy expenditure and peripheral glucose homeostasis. We report that the combined inactivation of PTP1B and TCPTP and the promotion of leptin and insulin signaling in POMC neurons promotes WAT browning and energy expenditure and prevents the development of diet-induced obesity. Our findings identify a novel mechanism in which POMC neurons integrate insulin and leptin feedback to drive WAT browning and maintain energy homeostasis.

RESULTS

Decreased adiposity in POMC-TC mice

Previous studies have established that PTP1B regulates leptin signaling in POMC neurons (Banno et al., 2010), but the precise neuronal populations in which TCPTP exerts its effects remain unknown. Thus, we assessed TCPTP versus GFP expression in the hypothalami of *Pomc*-GFP transgenic mice (Fig 1a; Fig S1a). TCPTP protein was detected in 39.7 ± 5.2% of all GFP positive POMC neurons in the ARC with co-localisation predominating in the central-caudal ARC (Fig 1b), where both LEPR- and IR-responsive POMC neurons have been detected (Williams et al., 2010). No TCPTP staining was detected in the rostral ARC (Fig S1b). The extent to which TCPTP colocalised with GFP expressing POMC neurons was confirmed by flow cytometry in papain-digested hypothalami (Fig 1c). LEPR-responsive POMC neurons are also found in the nucleus of the solitary tract (NTS) in the hindbrain. Although TCPTP expression was evident in the NTS, the majority of TCPTP staining did not colocalise with GFP-expressing POMC neurons (Fig S1c).

Next we examined the localisation of PTP1B in POMC neurons in the ARC and its coincidence with TCPTP (Fig 1d–f). PTP1B was detected in 74.8 ± 11.2% of all GFP-positive POMC neurons in the ARC, with PTP1B/GFP co-localisation predominating in the central-caudal ARC. In contrast to TCPTP, PTP1B was also expressed in the rostral ARC (Fig S1b). Moreover, PTP1B expression in the central-caudal ARC was not restricted to

medial POMC neurons, where it largely coincided with TCPTP (Fig 1f), but was also found in lateral POMC neurons, where TCPTP expression was not evident (Fig 1b, e). Also, TCPTP but not PTP1B was expressed in a subset of medial-caudal POMC neurons (Fig 1f). Thus, TCPTP and PTP1B are found in both overlapping and distinct POMC neuronal subsets in the ARC.

To determine whether TCPTP might function in the melanocortin pathway we crossed *Ptpn2*$^{fl/fl}$ mice (Loh et al., 2011) with *Pomc*-Cre transgenic mice, to excise *Ptpn2* (*Pomc*-Cre;*Ptpn2*$^{fl/fl}$: POMC-TC) in POMC-expressing neurons (Fig S1d–e). We compared these mice to PTP1B POMC neuronal cell-specific knockout mice (*Pomc*-Cre;*Ptpn1*$^{fl/fl}$: POMC-1B), generated as described previously (Banno et al., 2010). To visualise POMC cell-specific Cre-mediated recombination, we crossed POMC-TC mice to *Z/EG* reporter mice that express GFP after Cre-mediated recombination (Fig 1g). POMC-TC;*Z/EG* mice expressed GFP in the ARC and this overlapped with 92% of POMC expressing cells (Fig 1g–h); no GFP staining was evident in non-POMC cells. As reported for POMC-1B mice (Banno et al., 2010), no differences were evident in the number of hypothalamic POMC neurons in POMC-TC mice (Fig 1j). POMC is expressed in the ARC, as well as the pituitary and the NTS in the hindbrain. In addition, ARC POMC neurons project to the lateral reticular nucleus in the brainstem. Consistent with this, the recombined *Ptpn2* allele (Δ*Ptpn2*) in POMC-TC mice was evident in whole brain, hypothalamic, pituitary and hindbrain DNA extracts, but not in liver extracts (Fig S1d). As expected, differences in TCPTP protein were not observed in the hypothalamic extracts of POMC-TC versus control mice (Fig S1e), because POMC neurons constitute only a small proportion of the total hypothalamic cell population (Cowley et al., 2001).

Body weights were not altered in POMC-TC or POMC-1B versus floxed controls (Fig 2a; Fig S2a). Nevertheless, epididymal and subcutaneous fat pads weights were decreased in POMC-TC mice and trended lower in POMC-1B mice; only epididymal fat was significantly decreased in POMC-1B mice (Fig 2a–b). Moreover, dual energy X-ray absorptiometry (DEXA) revealed that whole body adiposity was significantly decreased in POMC-TC mice, but not in POMC-1B mice (Fig 2a–b). Neither bone mineral densities nor lean masses were altered (Fig 2a–b), and body lengths and liver weights were similar in both groups (Fig S2b–c). Previous studies have established that PTP1B deletion in the pituitary (*Cga*-Cre;*Ptpn1*$^{lox/lox}$) does not impact on body weight (Banno et al., 2010). Similarly, we found that TCPTP deletion in the pituitary (*Cga*-Cre;*Ptpn2*$^{lox/lox}$) did not result in overt differences in body weight or adiposity (Fig S2d–h). The differences in adiposity in POMC-TC and POMC-1B mice could not be ascribed to alterations in food intake, energy expenditure or activity and there were no differences in fuel utilisation (assessed by respiratory exchange ratio: RER) in either group (Fig S2i–j). These findings are consistent with previous studies reporting that LEPR or IR deficiencies in POMC neurons do not alter food intake or RER (Balthasar et al., 2004; Berglund et al., 2012; Hill et al., 2010; Konner et al., 2007).

PTP1B, but not TCPTP regulates leptin sensitivity

The deletion of TCPTP or PTP1B in neural and glial cells by Cre-LoxP recombination using the *Nes*-Cre transgene enhances leptin sensitivity and protects mice from diet-induced obesity (DIO) (Loh et al., 2011). Accordingly we assessed whether the decreased adiposity in chow-fed POMC-TC and POMC-1B mice might be ascribed to enhanced leptin sensitivity. POMC-TC, POMC-1B, or floxed control mice were administered leptin intraperitoneally (IP) for three days, and body weights and food intake were recorded. Surprisingly, deletion of TCPTP in POMC neurons did not alter the leptin-mediated attenuation of food intake or decrease in body weight (Fig 2c; Fig S2k), despite the fact that 86.5 ± 6.5 % of LEPR positive ARC POMC neurons express TCPTP (Fig S1f). In addition, plasma leptin levels (Fig 2d), leptin-induced STAT3 Y705 phosphorylation (p-STAT-3; Fig S2l–m), and leptin-induced hypothalamic *Pomc* expression (Fig 2g) were not altered by TCPTP deficiency consistent with unaltered leptin sensitivity. As reported previously (Banno et al., 2010), PTP1B deficiency enhanced the leptin-mediated repression of body weight (Fig 2e) without overt changes in food intake (Fig S2k), reduced fed plasma leptin levels (Fig 2f) and significantly increased leptin-induced hypothalamic p-STAT-3 and *Pomc* expression (Fig 2g; Fig S2n–o); as expected, there were no differences in *Agrp* and *Npy* expression (Fig S2p). Thus, the reduced adiposity in POMC-TC mice is independent of changes in leptin sensitivity.

TCPTP, but not PTP1B regulates insulin signaling

PTP1B and TCPTP dephosphorylate the IR and attenuate insulin signaling in the periphery (Tiganis, 2013). As the CNS effects of leptin and insulin overlap, and hypothalamic IR activation alters peripheral lipid and glucose metabolism (Marino et al., 2011; Plum et al., 2006), we monitored the effects of TCPTP versus PTP1B deficiency on hypothalamic insulin signaling. First, we determined whether PTP1B- vs. TCPTP-deficiency in POMC neurons enhanced insulin-induced PI3K/AKT signaling in the ARC by monitoring AKT Ser-473 phosphorylation (p-AKT) by immunohistochemistry. TCPTP, but not PTP1B, deficiency enhanced p-AKT staining in the ARC in response to insulin (Fig 2h–j). In keeping with the selective effects on p-AKT signaling, insulin-induced hypothalamic *Pomc* expression was significantly enhanced in POMC-TC, but not POMC-1B mice (Fig 2k). To independently assess TCPTP's capacity to regulate insulin signaling in POMC neurons we took advantage of a highly specific TCPTP inhibitor, compound 8 (Zhang et al., 2009). This inhibitor is highly selective for TCPTP over PTP1B and intracerebroventricular (ICV) compound 8 administration enhances leptin signaling and sensitivity in wild type mice, but not neuronal cell-specific TCPTP knockout mice (Loh et al., 2011). Compound 8 or aCSF (artificial cerebrospinal fluid) vehicle control were administered ICV into fasted C57BL/6 mice that were subsequently injected with insulin and hypothalami extracted for analysis by real time PCR. Administration of compound 8 increased insulin-induced *Pomc* expression by ~2.5 fold (Fig 2l). Taken together these results demonstrate that TCPTP attenuates insulin signaling in POMC neurons.

Decreased adiposity and increased energy expenditure in DKO mice

Our results indicate that PTP1B and TCPTP differentially contribute to leptin and insulin signaling in POMC neurons. Hence we generated POMC-TC and POMC-1B double knockout (DKO) mice to examine whether the combined increase in IR and LEPR signaling in POMC neurons affects body weight and glucose metabolism. DKO mice had a modest reduction in body weight at 10 weeks of age but body length, liver weight, lean mass and bone density were unaltered (Fig 3a–c). Differences in body weight could be explained by reduced whole-body adiposity (Fig 3b–c). The reduction in body weight and adiposity in DKO mice was accompanied by increased dark-phase energy expenditure without significant changes in ambulatory activity or RER (Fig 3d), or changes in food intake or feeding efficiency (Fig 3d). Furthermore, leptin sensitivity, as assessed by the effects of leptin on body weight (Fig 3e), or inferred by the reduced fed plasma leptin levels, was improved in DKO mice (Fig 3f). This was accompanied by increased leptin-induced hypothalamic *Pomc* expression in DKO mice (Fig 3g). Finally, insulin-induced hypothalamic *Pomc* expression was also increased in DKO mice (Fig 3h). These results are consistent with combined deficiencies in PTP1B and TCPTP promoting both central leptin and insulin signaling in POMC neurons to attenuate body weight/adiposity.

Increased BAT thermogenesis and WAT browning in DKO mice

As the decreased adiposity and increased energy expenditure in chow-fed DKO mice could not be accounted for by changes in food intake or ambulatory activity, we examined whether DKO mice had elevated BAT thermogenesis and/or WAT browning. Although interscapular BAT mass was not altered (Fig S3a), *Ucp-1* gene expression was increased by more than 3-fold in DKO mice consistent with increased BAT activity (Fig 4a); BAT *Ucp-1* expression was not altered in POMC-TC or POMC-1B mice (Fig 4a). Indeed BAT thermogenesis, as assessed with sensors implanted below interscapular BAT, was increased during the light phase (when mice are less active) in DKO mice, but not in POMC-TC, or POMC-1B mice (Fig 4b). On the other hand, core temperature was not different from controls (Fig S3b), consistent with normal whole-body thermoregulation.

To determine whether WAT browning was also elevated in DKO mice, we measured *Ucp-1* gene expression in epididymal, inguinal, mesenteric and infrarenal fat (Fig 4a). *Ucp-1* expression was increased by 15–20-fold, specifically in inguinal WAT in DKO mice; inguinal *Ucp-1* expression was not altered in POMC-TC or POMC-1B mice (Fig 4a). Elevated *Ucp-1* mRNA in the inguinal fat of DKO mice was accompanied by increases in UCP-1 protein (Fig 4c–d). Inguinal fat in DKO mice had a distinct histological [hematoxylin and eosin (H&E) staining] morphology (Fig 4e), characterised by the presence of small adipocyte clusters with a multilocular lipid droplet morphology, a characteristic of brown fat (Rosen and Spiegelman, 2014). WAT browning in DKO mice also was accompanied by increased expression of *Prdm16* and *Cidea* (Fig 4f), which are found in brown and beige adipocytes, and *Tmem26* and *Cd137* (Fig 4f), which are specific to beige adipocytes (Wu et al., 2012). Previous studies have shown that cold-induced WAT browning is associated by increased angiogenesis (Xue et al., 2009). We found that angiogenesis, assessed with the angiogenesis marker CD34, was significantly elevated in inguinal WAT in DKO mice (Fig

S3c–d). Together, these results demonstrate that the combined deletion of PTP1B and TCPTP in POMC neurons drives BAT thermogenesis and WAT browning.

SNA-dependent WAT browning decreases adiposity

To determine whether the increased WAT browning in DKO mice might be associated with SNA resulting from the combined deletion of PTP1B and TCPTP in POMC neurons, we assessed tyrosine hydroxylase (TH) expression in the inguinal fat of chow-fed DKO versus control mice. TH is the rate-limiting enzyme in catecholamine synthesis and a marker of sympathetic innervation and was elevated in the inguinal fat of DKO mice (Fig S3e–f). Next, to determine whether the increased SNA was responsible for the WAT browning, we asked whether sympathetic denervation might attenuate WAT browning in DKO mice. To this end we injected the neurotoxin 6-hydroxydopamine (6-OHDA) unilaterally into the inguinal fat area of 10 week-old DKO mice and monitored for changes in browning two weeks later. Unilateral sympathetic denervation dramatically reduced TH staining and attenuated WAT browning when compared with the contralateral fat pad, as assessed by gross morphology, the expression of browning genes (*Ucp-1*, *Pgc1α*, *Prdm16*, *Cidea*) and histology (Fig 5a–c) without affecting BAT *Ucp-1* expression (Fig 5d). Indeed, unilateral sympathetic denervation reverted the increased inguinal WAT *Ucp-1* levels in DKO mice to levels comparable to floxed control mice (Fig 5e). These results indicate that WAT browning in DKO mice is dependent on SNA, rather than changes in metabolism or circulating factors associated with the decreased adiposity.

Next, we sought to determine the extent to which the increased SNA to inguinal fat and consequent browning may contribute to the increased energy expenditure and decreased adiposity in DKO mice. We first asked whether WAT browning and/or BAT activity might precede the decreased body weight/adiposity evident in DKO mice. Increased WAT browning was evident as early as 4 weeks of age, prior to any differences in body weight or adiposity (Fig 4c, e–f, h). Moreover, the increased WAT browning in 4 week-old mice preceded changes in BAT activity, as assessed by the expression of *Ucp-1* (Fig 4g). To directly test that WAT browning decreased adiposity in DKO mice we bilaterally denervated the inguinal fat pads of chow-fed DKO mice using 6-OHDA and measured the effect on adiposity and browning after 5 weeks. Strikingly, sympathetic denervation in DKO mice (assessed by TH staining; Fig S3g) resulted in increased weight gain and adiposity (Fig 5f–g; Fig S4a). Importantly, the increased adiposity in denervated DKO mice was accompanied by a reduction in energy expenditure and decreased WAT browning (Fig 5h–i), without alterations in RER or ambulatory activity (Fig S4b). Moreover, the increased weight gain occurred despite BAT activity remaining elevated in DKO mice (Fig 5h). Taken together these results causally link the increased energy expenditure and decreased adiposity in DKO mice to the elevated WAT browning.

DKO mice are resistant to DIO

To assess the impact of combined PTP1B and TCPTP deficiencies in POMC neurons and increased WAT browning on DIO, we administered a high fat diet to POMC-TC, POMC-1B, or DKO mice for 12 weeks and monitored the effects on body weight and glucose metabolism (Fig 6, Supp. Figs 5–7). DKO mice exhibited a significant reduction in

weight gain and a marked reduction in adiposity (Fig 6a–c; Fig S7a). By contrast, no differences were observed in body weight, adiposity or energy expenditure in POMC-1B, or POMC-TC mice (Fig S5a–d; Supp. Fig 6a–d). The decreased weight gain in DKO mice was not associated with any difference in body length, lean mass or bone density (Fig 6c–d), but liver weights were significantly reduced and accompanied by a marked reduction in steatosis (Fig 6e). The decreased adiposity in high fat fed (HFF) DKO mice was accompanied by unaltered food intake, but feeding efficiency was increased consistent with improved energy utilisation. Moreover, HFF DKO mice exhibited increased oxygen consumption and energy expenditure, increased ambulatory activity and increased dark-phase RER (Fig 6f). In keeping with the resistance to DIO, DKO mice had significantly greater leptin sensitivity (Fig 6g). Moreover, DKO mice exhibited a significant reduction in fasted blood glucose levels and a trend for reduced fasted insulin levels and had improved insulin and glucose tolerances (Fig 6h–j; Fig S7b–c) consistent with overall improved glucose homeostasis. By contrast, HFF POMC-TC and POMC-1B single mutant mice did not exhibit any differences in leptin sensitivity and glucose homeostasis (Fig S5e–i; Fig S6e–i). These results demonstrate that the combined deletion of PTP1B and TCPTP in POMC neurons prevents the development of DIO and the associated insulin resistance, glucose intolerance and hepatosteatosis.

The decreased adiposity in HFF DKO mice was accompanied by elevated BAT *Ucp-1* expression and increased inguinal WAT browning (Fig 6k–m). To determine the extent to which the increased WAT browning in DKO mice prevented DIO, we bilaterally denervated (6-OHDA) the inguinal fat of DKO mice that had been HFF for 3 weeks and measured effects on adiposity, energy expenditure and glucose homeostasis after a further 5 weeks of high fat feeding (Fig 6n–o; Fig S7d–j). Bilaterally denervating inguinal fat in HFF DKO mice increased weight gain and adiposity (Fig 6n; Fig S7d–e). The increased weight gain was associated with decreased energy expenditure and RER, but no alterations in ambulatory activity or food intake (Fig 6o; Fig S7f). Moreover, the increased weight gain in the denervated HFF DKO mice was accompanied by elevated fasted blood glucose levels, insulin resistance, glucose intolerance and hepatosteatosis (Fig S7g–j). These results demonstrate that the resistance to DIO in HFF DKO mice can be attributed at least in part to increased WAT browning.

Insulin and leptin promote WAT browning in DKO mice

Our studies indicate that mice lacking PTP1B or TCPTP in POMC neurons exhibit enhanced leptin or insulin signaling respectively and that their combined deficiency increases WAT browning and energy expenditure to decrease adiposity. Although these results are consistent with enhanced insulin and leptin signaling driving WAT browning, they do not exclude the contribution of other pathways. Moreover, they do not exclude the possibility that the combined PTP1B and TCPTP deficiency may lead to synergistic effects on leptin-induced JAK2 activation and STAT-3 signaling, so that leptin signaling alone promotes WAT browning. To test this we administered POMC-1B (leptin hypersensitive) or POMC-TC (insulin hypersensitive) mice either vehicle or leptin and assessed the effects on body weight, WAT browning and BAT activity (Fig 7a–b). We reasoned that if both leptin and insulin signaling is required in POMC neurons for WAT browning, then WAT browning

would be greatest in the leptin-treated POMC-TC mice, as POMC-TC mice are insulin hypersensitive. On the other hand, if the exacerbation of leptin signaling by combined PTP1B and TCPTP deficiencies would be sufficient to drive browning, then this would be greatest in POMC-1B mice that are leptin hypersensitive. POMC-TC, POMC-1B or floxed control mice were administered leptin on a daily basis for six days and body weights, WAT browning and BAT *Ucp-1* expression assessed. POMC-1B mice exhibited the greatest decrease in body weight in response to leptin (Fig 7a). Consistent with the previously established potential for leptin to drive BAT thermogenesis, BAT *Ucp-1* was elevated in leptin-treated control mice (as compared to vehicle administered C57BL/6 mice), but this was not increased further by PTP1B or TCPTP-deficiency (Fig 7b). Leptin administration also modestly increased inguinal WAT browning (Fig 7b). However, browning was greatest for leptin-treated POMC-TC mice (Fig 7b–c; Fig S4c–d). Thus, the enhanced insulin and leptin signaling in POMC neurons may underlie the WAT browning and consequent increased energy expenditure and decreased adiposity in DKO mice.

Insulin and leptin act on ARC neurons to drive WAT browning

To directly assess the capacity of insulin and leptin to act synergistically in the CNS to control WAT browning we subcutaneously implanted osmotic minipumps to ICV administer either vehicle, leptin, insulin, or leptin plus insulin into the lateral ventricle over six days and monitored body weight, energy expenditure, BAT activity and WAT browning (Fig 7d–g). We found that insulin infusion alone had no effect on food intake or body weight (Fig 7d; Fig S4f). This is in keeping with previous studies demonstrating that the chronic ICV administration of insulin does not alter food intake or overall body weight (Koch et al., 2008). As expected, leptin decreased body weight and adiposity and notably, this was exacerbated by the co-infusion of insulin (Fig 7d). Co-infusion of leptin and insulin did not further reduce food intake compared to leptin only infusion (Fig S4f). To assess whether the synergistic effects of insulin and leptin on body weight may result from SNA-dependent WAT browning and/or BAT thermogenesis, we measured the expression of thermogenic genes in BAT and inguinal fat. We found 1) that BAT *Ucp-1* expression increased similarly in response to all treatments, but not by insulin alone (Fig 7e), and 2) leptin but not insulin treatment alone resulted in a modest increase in the expression of browning genes in inguinal fat (Fig 7e). In keeping with this, leptin alone modestly increased TH and UCP-1 in inguinal fat and increased whole body energy expenditure (Fig 7f–g; Fig S4h). However the co-infusion of leptin and insulin resulted in a marked increase in TH staining and WAT browning (Fig 7e–f; Fig S4e–h). Moreover, the co-infusion of leptin plus insulin resulted in a greater increase in energy expenditure than the infusion of leptin alone (Fig 7g), consistent with the difference in energy expenditure being attributable to increased WAT browning.

To determine the extent to which the leptin plus insulin-induced increase in energy expenditure and weight loss may be reliant on SNA-dependent WAT browning, we bilaterally denervated (6-OHDA) the inguinal fat pads of mice that were ICV infused with leptin plus insulin. We found that the increased WAT browning (*Ucp-1* expression) and energy expenditure and decreased body weight resulting from the co-infusion of leptin and insulin were significantly attenuated by the bilateral denervation of inguinal fat (Fig 7h–j). However, the denervation did not completely prevent the increase in energy expenditure and

decrease in body weight, probably because of the sustained leptin-induced activation of BAT and the suppression of food intake (Fig 7e, h, j; Supp Fig 4f).

Next, we assessed whether the effects of the ICV administered insulin and leptin on WAT browning may be mediated via neurons in the ARC. Moreover, since both insulin and leptin can signal via PI3K to depolarise and activate POMC neurons (Cowley et al., 2001; Hill et al., 2008; Qiu et al., 2010; Qiu et al., 2014; Rahmouni et al., 2004), we determined if the pharmacological inhibition of PI3K could suppress WAT browning. Minipumps and intra-ARC indwelling bilateral cannulas were used to infuse either vehicle, leptin plus insulin or leptin, insulin plus the PI3K inhibitor LY294002 directly into the ARC over six days and effects on body weight and WAT browning were monitored (Fig 7k–m; Fig S4i). The infusion of leptin/insulin directly into the ARC decreased body weight and food intake and promoted WAT browning and these effects were attenuated by LY294002 (Fig 7k–m; Fig S4i). Taken together these results demonstrate that insulin and leptin act synergistically on cells in the ARC, at least in part via PI3K, to increase WAT browning and consequent energy expenditure to decrease body weight.

ARC POMC neurons promote WAT browning

We next sought to understand how leptin and insulin elicit synergistic effects on ARC cells to promote WAT browning. Previous studies have provided evidence for the existence of distinct ARC POMC neurons that are differentially responsive to insulin and leptin (Hill et al., 2010; Williams et al., 2010). To determine if insulin and leptin may promote browning by stimulating different POMC neurons, we administered mice insulin, leptin, or insulin plus leptin intraperitoneally and monitored for hypothalamic STAT3 Y705 or AKT Ser-473 phosphorylation by immunohistochemistry (Fig S4j–l). Leptin stimulation resulted in p-AKT and p-STAT-3 staining in both the ARC and DMH, whereas insulin increased p-AKT largely in the ARC (Fig S4j). Strikingly, insulin plus leptin stimulation resulted in p-AKT staining in ARC neurons that were devoid of p-STAT-3 (Fig S4j–k). At least a subset of the cells staining for p-AKT only also stained for POMC-derived α-MSH (Fig S4l). Thus, insulin and leptin can stimulate distinct neurons in the ARC. Therefore, these results are consistent with the insulin plus leptin-mediated promotion of WAT browning resulting from the increased engagement of POMC neurons.

To assess if the leptin/insulin synergy reflects the increased recruitment of POMC neurons to the melanocortin response we sought to non-selectively activate ARC POMC neurons with the stimulatory hM3Dq DREADD (designer receptors exclusively activated by designer drugs) that is activated by clozapine-N-oxide (CNO) (Krashes et al., 2011). rAAV-hM3Dq-mCherry (capable of expressing hM3Dq-mCherry in a Cre-dependent manner) was administered into the ARC of 10 week-old *Pomc*-Cre mice that were subsequently unilaterally denervated (inguinal fat pads) with 6-OHDA. Mice were then administered vehicle or CNO, to depolarise POMC neurons, and body weights and food intake measured and WAT browning assessed after 14 days. CNO decreased food intake and body weight consistent with POMC neuronal activation (data not shown). Post-mortem analysis confirmed ARC targeting and mCherry expression in 73.1 ± 20.7% of POMC neurons (Fig S4m–n). CNO administration resulted in a marked increase in WAT browning in the sham-

operated contralateral inquinal fat pads, but not in the 6-OHDA denervated inguinal fat pads (Fig 7n–p). These results demonstrate that the non-selective activation of ARC POMC neurons promotes the SNA-dependent browning of inguinal WAT. This is consistent with the synergistic actions of insulin and leptin on WAT browning reflecting the increased engagement and activation of POMC neurons.

DISCUSSION

Our studies demonstrate that leptin and insulin act synergistically on hypothalamic POMC neurons to promote WAT browning and energy expenditure to decrease adiposity. We suggest that the engagement of both insulin- and leptin-responsive POMC neurons might allow for a graded melanocortin response to regulate fat stores. Leptin would elicit immediate effects on food intake, ambulatory activity and energy expenditure by promoting BAT activity, whereas leptin and heightened postprandial insulin would act synergistically over the longer term and engage a greater proportion of POMC neurons to promote overt WAT browning and increase energy expenditure to limit weight gain. This may be a major factor contributing to the ‘diet-induced thermogenesis’ model of body weight control, as first described by Rothwell and Stock in 1979, whose studies involved BAT cellular expansion and differentiation in rodents eating a cafeteria diet (Rothwell and Stock, 1979).

We found that TCPTP was expressed in 40% and PTP1B in 70% of ARC POMC neurons and that the two phosphatases differentially contributed to leptin and insulin signaling. Previous studies have established that both phosphatases can attenuate leptin and insulin signaling in varied cell types and tissues (Tiganis, 2013). Indeed, PTP1B attenuates insulin signaling in SF-1 neurons in the VMH (Chiappini et al., 2014), whereas neuronal/glial TCPTP deficiency promotes hypothalamic leptin signaling *in vivo* (Loh et al., 2011). In this study we found that PTP1B deficiency enhanced leptin, but not insulin signaling, and TCPTP-deficiency enhanced insulin, but not leptin signaling in POMC neurons. To some degree, the differential contributions of the phosphatases may be due to their segregation in distinct POMC neuronal subsets. PTP1B, but not TCPTP, was expressed in POMC neurons in the rostral ARC, whereas a significant proportion of lateral POMC neurons in the central-caudal ARC differentially expressed PTP1B and TCPTP. This is reminiscent of studies supporting the existence of distinct subsets of POMC neurons and insulin versus leptin-responsive POMC neurons in the ARC (Hill et al., 2010; Sohn et al., 2011; Williams et al., 2010), and supported by our findings demonstrating that insulin and leptin can signal via distinct ARC/POMC neurons. However, despite a significant degree of segregation, PTP1B and TCPTP were co-expressed in medial POMC neurons in the central-caudal ARC, and TCPTP was expressed in the majority of LEPR-expressing POMC neurons. Therefore, the impact of PTP1B- versus TCPTP-deficiency on leptin versus insulin signaling and that of their combined deficiencies on WAT browning and energy expenditure may also be ascribed at least in part to functional redundancies, with PTP1B predominating in leptin and TCPTP in insulin signaling.

Irrespective of the roles of PTP1B and TCPTP, our findings demonstrate that both insulin and leptin are required for optimal CNS-mediated WAT browning. First, daily leptin administration modestly increased browning in floxed control and leptin hyper-responsive

POMC-1B mice, however overt WAT browning was only evident in insulin hyper-responsive POMC-TC mice. Second, leptin or insulin ICV infusion alone had little effect on browning, respectively, whereas the co-infusion of insulin and leptin strikingly enhanced browning. In contrast to WAT browning, we found that BAT activity was enhanced by 2–3 fold in response to leptin, but not insulin, and was not enhanced further by co-infusion of leptin and insulin. Previous studies have implicated ARC/POMC neurons and/or leptin-induced PI3K signaling in BAT thermogenesis and WAT browning (Commins et al., 2000; Plum et al., 2007; Sasaki et al., 2013; Williams et al., 2014). However, our studies demonstrate directly that POMC neuronal activation promotes SNA-dependent WAT browning, and that insulin and leptin can act synergistically on POMC neurons to promote browning that far exceeds that achieved with leptin alone. Moreover, our studies provide evidence for the differential central control of BAT activity versus WAT browning and thus ascribe distinct physiological functions to these thermogenic tissues.

The importance of beige adipocytes to body weight control is underscored by studies overexpressing or deleting the brown adipose tissue determination factor *Prdm16* in fat (Cohen et al., 2014; Seale et al., 2011). In keeping with the overall importance of WAT browning for thermogenesis and energy expenditure, previous studies have shown that beige adipocytes can increase their energy uptake similar to BAT in the context of cold exposure or β_3-adenergic stimulation (Bartelt et al., 2011; Bartelt and Heeren, 2014). Moreover the thermogenic capacity of mitochondria isolated from the inguinal fat of cold-acclimated mice is roughly one third of that of interscapular BAT (Shabalina et al., 2013). Our own studies highlight the critical importance of CNS mediated WAT browning to regulate body weight and adiposity independently of BAT thermogenesis and highlight the importance of WAT browning in the prevention of diet-induced obesity.

In summary, our findings define the complementary roles of TCPTP and PTP1B in central insulin and leptin signaling in POMC neurons and the synergistic central actions of insulin and leptin in the promotion of WAT browning. Our results suggest that browning may be the outcome of an integrated melanocortin response to peripheral factors that convey the status of both current (conveyed by leptin) and anticipated energy reserves (conveyed by increases in insulin).

EXPERIMENTAL PROCEDURES

Mice

We maintained mice on a 12 h light-dark cycle in a temperature-controlled high barrier facility with free access to food and water. Mice were fed a standard chow (4.6% fat) or a high-fat diet (23% fat; 45% of total energy from fat; SF04-027; Specialty Feeds) as indicated. Experiments were approved by the Monash University School of Biomedical Sciences Animal Ethics Committee.

Immunohistochemistry

Immunohistochemistry to monitor for p-STAT3 and p-AKT in hypothalamic neurons was performed as described previously (Loh et al., 2011) and staining for TCPTP, PTP1B, eGFP

and POMC performed as described in *Extended Experimental Procedures*. For inguinal WAT immunohistochemistry tissue was formalin-fixed and processed for UCP-1, CD34 or TH immunoreactivity as described in *Extended Experimental Procedures*.

Metabolic measurements

Insulin and glucose tolerance tests, leptin sensitivity, blood glucose and plasma insulin measurements were performed as described previously (Loh et al., 2009). Activity, food intake and energy expenditure were assessed using a Comprehensive Lab Animal Monitoring System (Columbus Instruments), and body composition determined by DEXA (Lunar PIXImus2; GE Healthcare).

Real-time PCR

RNA was extracted using TRIzol reagent (Sigma), reverse transcribed and processed for quantitative (ΔΔCt) real-time PCR using either TaqMan Gene Expression Assays (Applied Biosystems) or SsoAdvanced Universal SYBR Green Supermix (BioRad) as described in *Extended Experimental Procedures*.

BAT and core temperature measurements

BAT and core temperatures and locomotor activity were measured as described previously (Enriori et al., 2011). E-Mitters (Mini Mitter Company) were implanted beneath the BAT pad between the scapulae or into the peritoneal cavity.

Sympathetic denervation

Mice received 20 microinjections of vehicle or 6-hydroxydopamine [6-OHDA (Sigma); 1 μl per injection, 9 mg/ml in 0.15 M NaCl containing 1% (w/v) ascorbic acid] as described previously (Chao et al., 2011) throughout the right or both inguinal fat pads.

Intracerebroventricular and intra-ARC infusions

8-week-old C57BL/6 mice were implanted with a sterile osmotic pump and connector cannula (Alzet Brain Infusion Kit 3, DURECT Corp) as described in Supplemental Experimental Procedures For intra-ARC infusions mice were implanted with a bilateral cannula (Plastics One Inc.) 1.4 mm caudal of bregma, extending 5.7 mm below dura, connected to a minipump (Alzet model 1002, DURECT Corp) via PEG tubing and a Y connector. Mice received 6-day infusions of vehicle, leptin (200 ng/h equating to 4.8 μg/day, Peprotech), human insulin (125 μU/h, 3 mU/day, Sigma) or leptin plus insulin and body weights and food intake monitored and tissues extracted.

DREADD

10–12 week-old *Pomc*-Cre mice were sterotaxically injected with rAAV-hSyn-DIO-hM3D(Gq)-mCherry bilaterally into the ARC (coordinates, bregma: anterior-posterior, −1.40 mm; dorsal-ventral, −5.80 mm; lateral, +/−0.30 mm, 200 nl/side) as described previously (Krashes et al., 2011). Two weeks after rAAV delivery mice were unilaterally denervated with 6-OHDA. One week post denervation mice received daily injections of vehicle or CNO (1.5 mg/kg, IP, Sigma) for 14 days. Body weights and food intake were

recorded. Mice were anaesthetised, tissues extracted and mice perfused with paraformaldehyde for immunohistochemical assessment.

Statistical analysis

Unless otherwise indicated statistical significance was determined by a two-tailed paired Student's t-test. P values <0.05 were considered significant; * $p<0.05$, ** $p<0.01$, *** $p<0.001$.

Supplementary Material

Refer to Web version on PubMed Central for supplementary material.

Acknowledgments

This work was supported by the NHMRC of Australia (to TT, ZBA, MAC), the NIH (to BGN (R37-CA49152), Z-YZ [RO1-CA126937], KKB [RO1-DK082417] and BBK [P01 DK56116]), and funds from the Ontario Ministry of Health and Long Term Care and the Princess Margaret Cancer Foundation (BGN).

References

Balthasar N, Coppari R, McMinn J, Liu SM, Lee CE, Tang V, Kenny CD, McGovern RA, Chua SC Jr, Elmquist JK, et al. Leptin receptor signaling in POMC neurons is required for normal body weight homeostasis. Neuron. 2004; 42:983–91. [PubMed: 15207242]

Banno R, Zimmer D, De Jonghe BC, Atienza M, Rak K, Yang W, Bence KK. PTP1B and SHP2 in POMC neurons reciprocally regulate energy balance in mice. J Clin Invest. 2010; 120:720–34. [PubMed: 20160350]

Bartelt A, Bruns OT, Reimer R, Hohenberg H, Ittrich H, Peldschus K, Kaul MG, Tromsdorf UI, Weller H, Waurisch C, et al. Brown adipose tissue activity controls triglyceride clearance. Nat Med. 2011; 17:200–5. [PubMed: 21258337]

Bartelt A, Heeren J. Adipose tissue browning and metabolic health. Nat Rev Endocrinol. 2014; 10:24–36. [PubMed: 24146030]

Bence KK, Delibegovic M, Xue B, Gorgun CZ, Hotamisligil GS, Neel BG, Kahn BB. Neuronal PTP1B regulates body weight, adiposity and leptin action. Nat Med. 2006; 12:917–24. [PubMed: 16845389]

Benoit SC, Air EL, Coolen LM, Strauss R, Jackman A, Clegg DJ, Seeley RJ, Woods SC. The catabolic action of insulin in the brain is mediated by melanocortins. J Neurosci. 2002; 22:9048–52. [PubMed: 12388611]

Berglund ED, Vianna CR, Donato J Jr, Kim MH, Chuang JC, Lee CE, Lauzon DA, Lin P, Brule LJ, Scott MM, et al. Direct leptin action on POMC neurons regulates glucose homeostasis and hepatic insulin sensitivity in mice. J Clin Invest. 2012; 122:1000–9. [PubMed: 22326958]

Bostrom P, Wu J, Jedrychowski MP, Korde A, Ye L, Lo JC, Rasbach KA, Bostrom EA, Choi JH, Long JZ, et al. A PGC1-α-dependent myokine that drives brown-fat-like development of white fat and thermogenesis. Nature. 2012; 481:463–8. [PubMed: 22237023]

Bruning JC, Gautam D, Burks DJ, Gillette J, Schubert M, Orban PC, Klein R, Krone W, Muller-Wieland D, Kahn CR. Role of brain insulin receptor in control of body weight and reproduction. Science. 2000; 289:2122–5. [PubMed: 11000114]

Chao PT, Yang L, Aja S, Moran TH, Bi S. Knockdown of NPY expression in the dorsomedial hypothalamus promotes development of brown adipocytes and prevents diet-induced obesity. Cell Metab. 2011; 13:573–83. [PubMed: 21531339]

Chiappini F, Catalano KJ, Lee J, Peroni OD, Lynch J, Dhaneshwar AS, Wellenstein K, Sontheimer A, Neel BG, Kahn BB. Ventromedial hypothalamus-specific Ptpn1 deletion exacerbates diet-induced obesity in female mice. J Clin Invest. 2014; 124:3781–92. [PubMed: 25083988]

Cohen P, Levy JD, Zhang Y, Frontini A, Kolodin DP, Svensson KJ, Lo JC, Zeng X, Ye L, Khandekar MJ, et al. Ablation of PRDM16 and beige adipose causes metabolic dysfunction and a subcutaneous to visceral fat switch. Cell. 2014; 156:304–16. [PubMed: 24439384]

Coll AP, Farooqi IS, Challis BG, Yeo GS, O'Rahilly S. Proopiomelanocortin and energy balance: insights from human and murine genetics. J Clin Endocrinol Metab. 2004; 89:2557–62. [PubMed: 15181023]

Commins SP, Watson PM, Levin N, Beiler RJ, Gettys TW. Central leptin regulates the UCP1 and ob genes in brown and white adipose tissue via different beta-adrenoceptor subtypes. J Biol Chem. 2000; 275:33059–67. [PubMed: 10938091]

Cowley MA, Smart JL, Rubinstein M, Cerdan MG, Diano S, Horvath TL, Cone RD, Low MJ. Leptin activates anorexigenic POMC neurons through a neural network in the arcuate nucleus. Nature. 2001; 411:480–4. [PubMed: 11373681]

Cypess AM, Lehman S, Williams G, Tal I, Rodman D, Goldfine AB, Kuo FC, Palmer EL, Tseng YH, Doria A, et al. Identification and importance of brown adipose tissue in adult humans. N Engl J Med. 2009; 360:1509–17. [PubMed: 19357406]

Elias CF, Aschkenasi C, Lee C, Kelly J, Ahima RS, Bjorbaek C, Flier JS, Saper CB, Elmquist JK. Leptin differentially regulates NPY and POMC neurons projecting to the lateral hypothalamic area. Neuron. 1999; 23:775–86. [PubMed: 10482243]

Enriori PJ, Sinnayah P, Simonds SE, Garcia Rudaz C, Cowley MA. Leptin action in the dorsomedial hypothalamus increases sympathetic tone to brown adipose tissue in spite of systemic leptin resistance. J Neurosci. 2011; 31:12189–97. [PubMed: 21865462]

Hill JW, Elias CF, Fukuda M, Williams KW, Berglund ED, Holland WL, Cho YR, Chuang JC, Xu Y, Choi M, et al. Direct insulin and leptin action on proopiomelanocortin neurons is required for normal glucose homeostasis and fertility. Cell Metab. 2010; 11:286–97. [PubMed: 20374961]

Hill JW, Williams KW, Ye C, Luo J, Balthasar N, Coppari R, Cowley MA, Cantley LC, Lowell BB, Elmquist JK. Acute effects of leptin require PI3K signaling in hypothalamic proopiomelanocortin neurons in mice. J Clin Invest. 2008; 118:1796–805. [PubMed: 18382766]

Koch L, Wunderlich FT, Seibler J, Konner AC, Hampel B, Irlenbusch S, Brabant G, Kahn CR, Schwenk F, Bruning JC. Central insulin action regulates peripheral glucose and fat metabolism in mice. J Clin Invest. 2008; 118:2132–47. [PubMed: 18451994]

Konner AC, Janoschek R, Plum L, Jordan SD, Rother E, Ma X, Xu C, Enriori P, Hampel B, Barsh GS, et al. Insulin Action in AgRP-Expressing Neurons Is Required for Suppression of Hepatic Glucose Production. Cell Metab. 2007; 5:438–49. [PubMed: 17550779]

Krashes MJ, Koda S, Ye C, Rogan SC, Adams AC, Cusher DS, Maratos-Flier E, Roth BL, Lowell BB. Rapid, reversible activation of AgRP neurons drives feeding behavior in mice. J Clin Invest. 2011; 121:1424–8. [PubMed: 21364278]

Lee P, Linderman JD, Smith S, Brychta RJ, Wang J, Idelson C, Perron RM, Werner CD, Phan GQ, Kammula US, et al. Irisin and FGF21 are cold-induced endocrine activators of brown fat function in humans. Cell Metab. 2014; 19:302–9. [PubMed: 24506871]

Lidell ME, Betz MJ, Dahlqvist Leinhard O, Heglind M, Elander L, Slawik M, Mussack T, Nilsson D, Romu T, Nuutila P, et al. Evidence for two types of brown adipose tissue in humans. Nat Med. 2013; 19:631–4. [PubMed: 23603813]

Loh K, Deng H, Fukushima A, Cai X, Boivin B, Galic S, Bruce C, Shields BJ, Skiba B, Ooms LM, et al. Reactive oxygen species enhance insulin sensitivity. Cell Metab. 2009; 10:260–72. [PubMed: 19808019]

Loh K, Fukushima A, Zhang X, Galic S, Briggs D, Enriori PJ, Simonds S, Wiede F, Reichenbach A, Hauser C, et al. Elevated hypothalamic TCPTP in obesity contributes to cellular leptin resistance. Cell Metab. 2011; 14:684–99. [PubMed: 22000926]

Marino JS, Xu Y, Hill JW. Central insulin and leptin-mediated autonomic control of glucose homeostasis. Trends Endocrinol Metab. 2011; 22:275–85. [PubMed: 21489811]

Morrison SF, Madden CJ, Tupone D. Central neural regulation of brown adipose tissue thermogenesis and energy expenditure. Cell Metab. 2014; 19:741–56. [PubMed: 24630813]

Myers MG, Cowley MA, Munzberg H. Mechanisms of leptin action and leptin resistance. Annu Rev Physiol. 2008; 70:537–56. [PubMed: 17937601]

Ouellet V, Routhier-Labadie A, Bellemare W, Lakhal-Chaieb L, Turcotte E, Carpentier AC, Richard D. Outdoor temperature, age, sex, body mass index, and diabetic status determine the prevalence, mass, and glucose-uptake activity of 18F-FDG-detected BAT in humans. Journal Clin Endocrinol Metab. 2011; 96:192–9. [PubMed: 20943785]

Plum L, Belgardt BF, Bruning JC. Central insulin action in energy and glucose homeostasis. J Clin Invest. 2006; 116:1761–6. [PubMed: 16823473]

Plum L, Rother E, Munzberg H, Wunderlich FT, Morgan DA, Hampel B, Shanabrough M, Janoschek R, Konner AC, Alber J, et al. Enhanced leptin-stimulated PI3K activation in the CNS promotes white adipose tissue transdifferentiation. Cell Metab. 2007; 6:431–45. [PubMed: 18054313]

Qiu J, Fang Y, Ronnekleiv OK, Kelly MJ. Leptin excites proopiomelanocortin neurons via activation of TRPC channels. J Neurosci. 2010; 30:1560–5. [PubMed: 20107083]

Qiu J, Zhang C, Borgquist A, Nestor CC, Smith AW, Bosch MA, Ku S, Wagner EJ, Ronnekleiv OK, Kelly MJ. Insulin excites anorexigenic proopiomelanocortin neurons via activation of canonical transient receptor potential channels. Cell Metab. 2014; 19:682–93. [PubMed: 24703699]

Rahmouni K, Morgan DA, Morgan GM, Liu X, Sigmund CD, Mark AL, Haynes WG. Hypothalamic PI3K and MAPK differentially mediate regional sympathetic activation to insulin. J Clin Invest. 2004; 114:652–8. [PubMed: 15343383]

Rosen ED, Spiegelman BM. What we talk about when we talk about fat. Cell. 2014; 156:20–44. [PubMed: 24439368]

Rothwell NJ, Stock MJ. A role for brown adipose tissue in diet-induced thermogenesis. Nature. 1979; 281:31–5. [PubMed: 551265]

Ruan HB, Dietrich MO, Liu ZW, Zimmer MR, Li MD, Singh JP, Zhang K, Yin R, Wu J, Horvath TL, et al. O-GlcNAc transferase enables AgRP neurons to suppress browning of white fat. Cell. 2014; 159:306–17. [PubMed: 25303527]

Saltiel AR, Kahn CR. Insulin signalling and the regulation of glucose and lipid metabolism. Nature. 2001; 414:799–806. [PubMed: 11742412]

Seale P, Conroe HM, Estall J, Kajimura S, Frontini A, Ishibashi J, Cohen P, Cinti S, Spiegelman BM. Prdm16 determines the thermogenic program of subcutaneous white adipose tissue in mice. J Clin Invest. 2011; 121:96–105. [PubMed: 21123942]

Shabalina IG, Petrovic N, de Jong JM, Kalinovich AV, Cannon B, Nedergaard J. UCP1 in brite/beige adipose tissue mitochondria is functionally thermogenic. Cell Rep. 2013; 5:1196–203. [PubMed: 24290753]

Sohn JW, Xu Y, Jones JE, Wickman K, Williams KW, Elmquist JK. Serotonin 2C receptor activates a distinct population of arcuate proopiomelanocortin neurons via TRPC channels. Neuron. 2011; 71:488–97. [PubMed: 21835345]

Tiganis T. PTP1B and TCPTP - nonredundant phosphatases in insulin signaling and glucose homeostasis. FEBS J. 2013; 280:445–58. [PubMed: 22404968]

van Marken Lichtenbelt WD, Vanhommerig JW, Smulders NM, Drossaerts JM, Kemerink GJ, Bouvy ND, Schrauwen P, Teule GJ. Cold-activated brown adipose tissue in healthy men. N Engl J Med. 2009; 360:1500–8. [PubMed: 19357405]

Varela L, Horvath TL. Leptin and insulin pathways in POMC and AgRP neurons that modulate energy balance and glucose homeostasis. EMBO Rep. 2012; 13:1079–86. [PubMed: 23146889]

Virtanen KA, Lidell ME, Orava J, Heglind M, Westergren R, Niemi T, Taittonen M, Laine J, Savisto NJ, Enerback S, et al. Functional brown adipose tissue in healthy adults. N Engl J Med. 2009; 360:1518–25. [PubMed: 19357407]

Williams KW, Liu T, Kong X, Fukuda M, Deng Y, Berglund ED, Deng Z, Gao Y, Sohn JW, Jia L, et al. Xbp1s in pomc neurons connects ER stress with energy balance and glucose homeostasis. Cell Metab. 2014; 20:471–82. [PubMed: 25017942]

Williams KW, Margatho LO, Lee CE, Choi M, Lee S, Scott MM, Elias CF, Elmquist JK. Segregation of acute leptin and insulin effects in distinct populations of arcuate proopiomelanocortin neurons. J Neurosci. 2010; 30:2472–9. [PubMed: 20164331]

Wu J, Bostrom P, Sparks LM, Ye L, Choi JH, Giang AH, Khandekar M, Virtanen KA, Nuutila P, Schaart G, et al. Beige adipocytes are a distinct type of thermogenic fat cell in mouse and human. Cell. 2012; 150:366–76. [PubMed: 22796012]

Xue Y, Petrovic N, Cao R, Larsson O, Lim S, Chen S, Feldmann HM, Liang Z, Zhu Z, Nedergaard J, et al. Hypoxia-independent angiogenesis in adipose tissues during cold acclimation. Cell Metab. 2009; 9:99–109. [PubMed: 19117550]

Zhang S, Chen L, Luo Y, Gunawan A, Lawrence DS, Zhang ZY. Acquisition of a potent and selective TC-PTP inhibitor via a stepwise fluorophore-tagged combinatorial synthesis and screening strategy. J Am Chem Soc. 2009; 131:13072–9. [PubMed: 19737019]

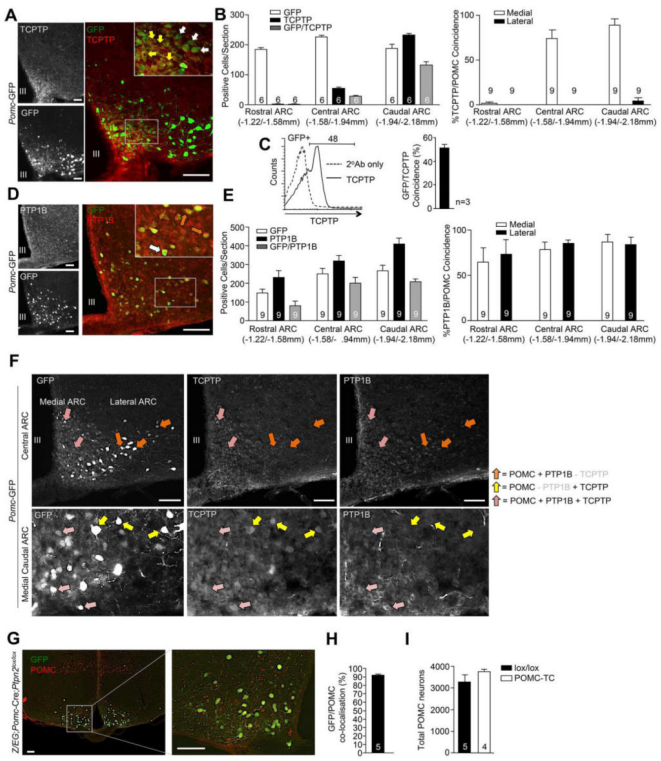

Figure 1. TCPTP and PTP1B in POMC neurons

a) Immunostaining for TCPTP in GFP+ ARC POMC neurons. **b)** Rostral-caudal immunostaining quantification of GFP and TCPTP expressing ARC cells. **c)** Papain-digested hypothalami of *Pomc*-GFP mice were analysed by flow cytometry for GFP and TCPTP. **d**) Immunostaining for PTP1B in GFP+ POMC neurons. **e)** Rostral-caudal immunostaining quantification of GFP and PTP1B expression in the ARC. **f)** Immunostaining for PTP1B and TCPTP in GFP positive POMC neurons in the ARC**. g)** Immunostaining and **h**, **i**) quantification of ARC GFP and POMC co-localisation and the total number of ARC POMC neurons in POMC-TC;*Z/EG* mice. Representative images of 3 or more experiments are shown. Data are means ± SEM for the indicated number of mice (30 sections/mouse), or (c) experimental repeats.

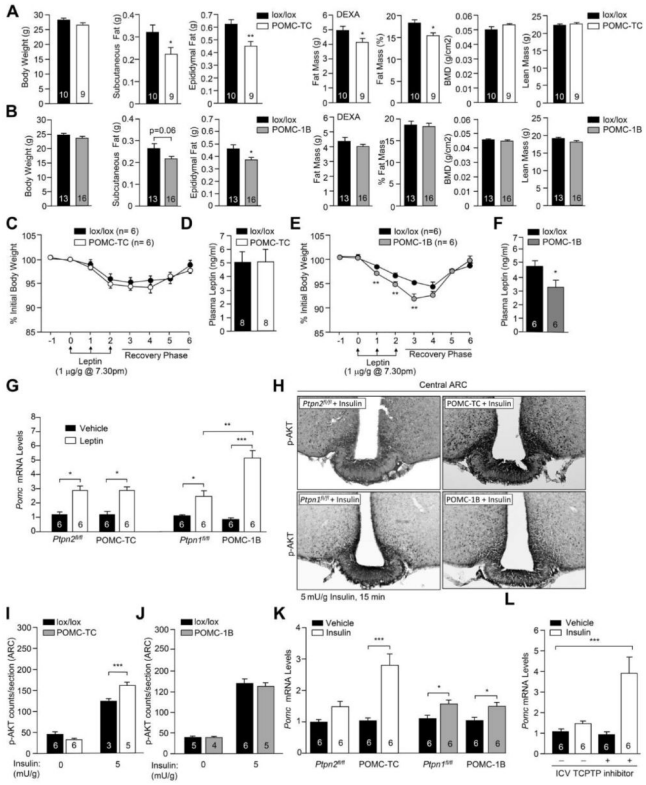

Figure 2. TCPTP and PTP1B regulate insulin and leptin signaling

a–b) Body and WAT weights and body composition in 10 week-old POMC-TC, POMC-1B and lox/lox mice. **(c & e)** POMC-TC, POMC-1B and lox/lox mice were administered leptin and body weights monitored. **d & f)** Fed plasma leptin levels. **g)** Hypothalamic *Pomc* gene expression in mice injected IP saline or leptin (1 μg/g, 2 h). **h–j)** p-AKT immunostaining in mice administered saline or insulin. **k)** Hypothalamic *Pomc* gene expression in mice injected IP saline or insulin (0.85 mU/g, 2 h). **l)** Hypothalamic *Pomc* gene expression in C57BL/6 mice administered saline or insulin (0.85 mU/g, IP, 2 h) followed by aCSF or TCPTP inhibitor [1.5 μl 0.2 nmol compound 8, ICV]. Results are means ± SEM and are representative of 3 independent experiments; significance determined using c, e, g–l) two-way, or m) one-way ANOVA.

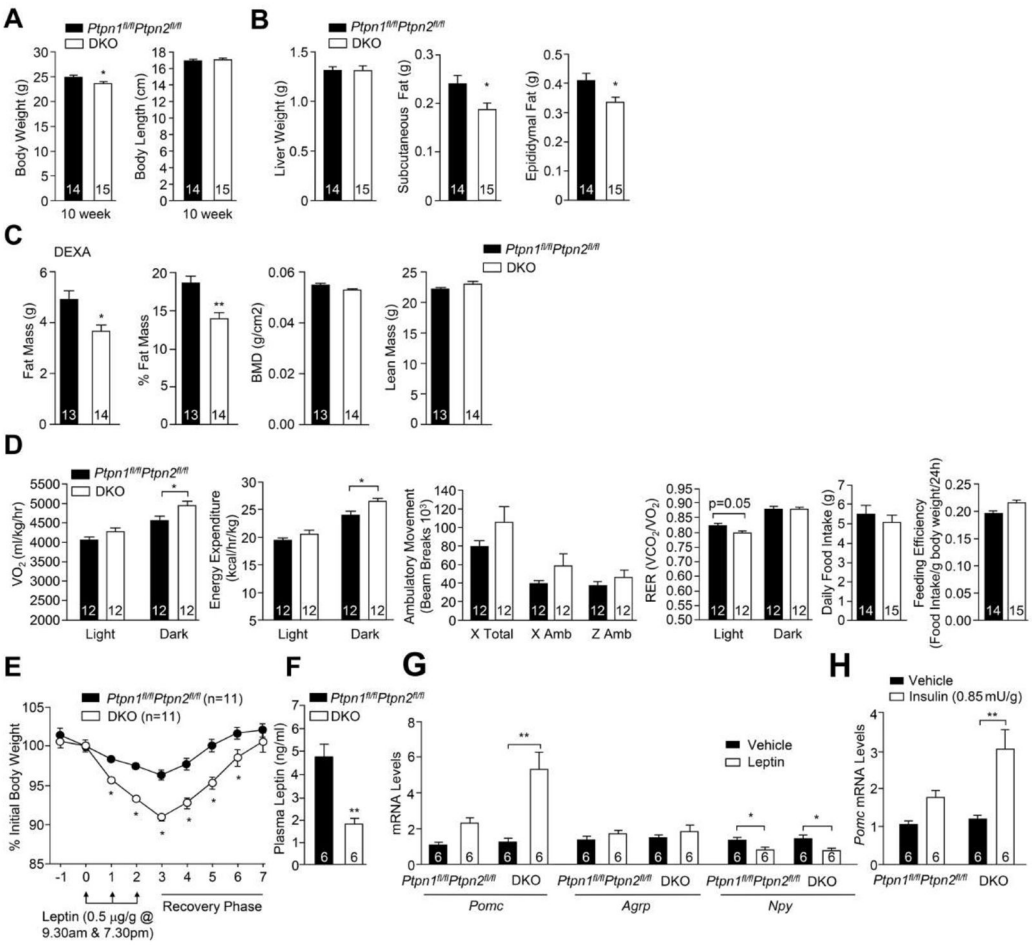

Figure 3. Decreased adiposity and increased energy expenditure in DKO mice

a) Body weight, body length, **b)** tissue weights, **c)** body composition, and **d)** oxygen consumption, energy expenditure, ambulatory activity, RER, daily food intake and feeding efficiency in 8–10 week-old DKO and *Ptpn1*$^{fl/fl}$*Ptpn2*$^{fl/fl}$ mice. **e)** Mice were administered leptin and body weights recorded. **f)** Fed plasma leptin levels. **g–h**) Hypothalamic gene expression in fasted mice injected IP saline, **g)** leptin, or **h)** insulin. Results are means ± SEM and are representative of at least 2 independent experiments; significance determined d–e, g–h) using two-way ANOVA.

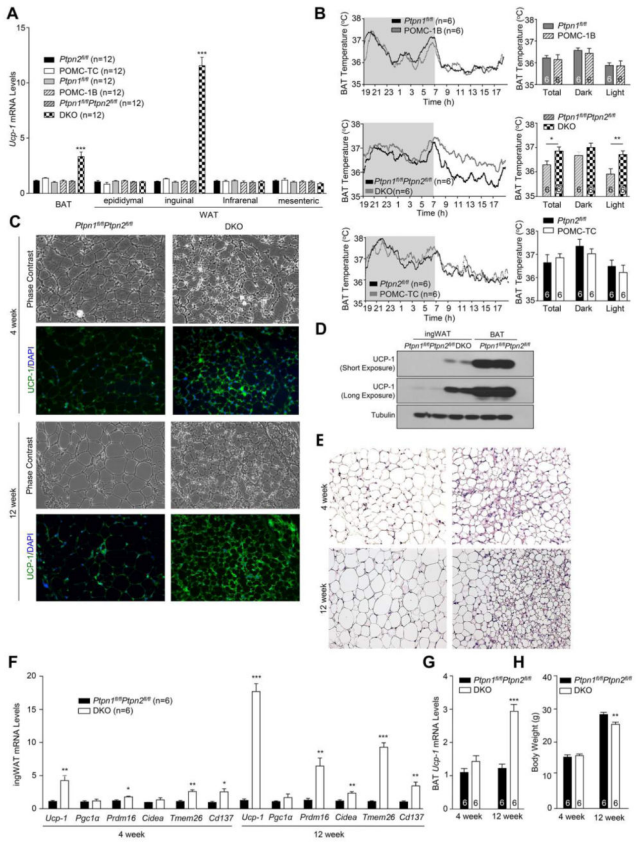

Figure 4. Increased browning in DKO mice

A) *Ucp-1* gene expression in BAT and WAT depots extracted from 12 week-old POMC-1B, POMC-TC, DKO and floxed control mice. **b)** Interscapular BAT temperatures. **c–e)** Histology (H&E), immunoblotting and UCP-1 immunohistochemistry in inguinal WAT (IngWAT). **f–g)** Browning gene expression in ingWAT or BAT and **h**) body weights. Data are means ± SEM and are representative of 3 independent experiments; significance determined using a) one-way, or, f–g) two-way ANOVA.

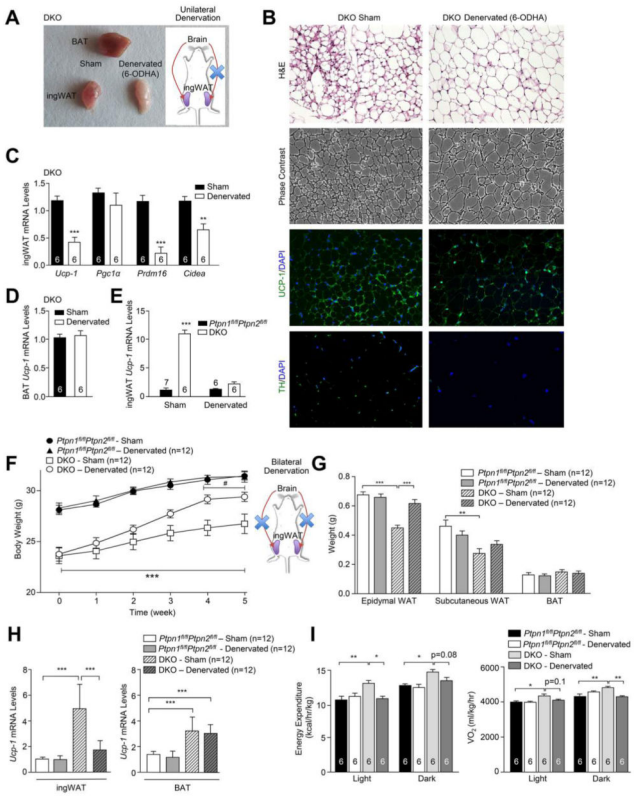

Figure 5. Denervation of DKO inguinal WAT and increases body weight

a–d) IngWAT **in** 10 week-old DKO mice was unilaterally denervated (6-ODHA) and BAT and ingWAT extracted 2 weeks later for analysis by **a**) gross morphology, **b**) histology, immunohistochemistry and **c–d**) real time PCR; vehicle administered contralateral inguinal fat pads were used as controls. **e)** Contralateral sham versus denervated (6-ODHA) ingWAT from DKO versus *Ptpn1*$^{fl/fl}$*Ptpn2*$^{fl/fl}$ mice was analysed for *Ucp-1* expression. **f–h)** 8 week-old *Ptpn1*$^{fl/fl}$*Ptpn2*$^{fl/fl}$ and DKO mice were sham-operated or bilaterally denervated and (**f**) body weights, **g**) BAT and WAT weights assessed and **h**) ingWAT and BAT *Ucp-1* expression measured. **i)** Energy expenditure and oxygen consumption in 24 week-old *Ptpn1*$^{fl/fl}$*Ptpn2*$^{fl/fl}$ and DKO mice 5 weeks after sham or bilateral ingWAT denervations. Data are means ± SEM and are representative of 3 independent experiments; significance determined using e–f) two-way, or g–i) one-way ANOVA. f) * corresponds to DKO v/s *Ptpn1*$^{fl/fl}$*Ptpn2*$^{fl/fl}$; $^{\#}$ denervated DKO v/s sham-operated DKO.

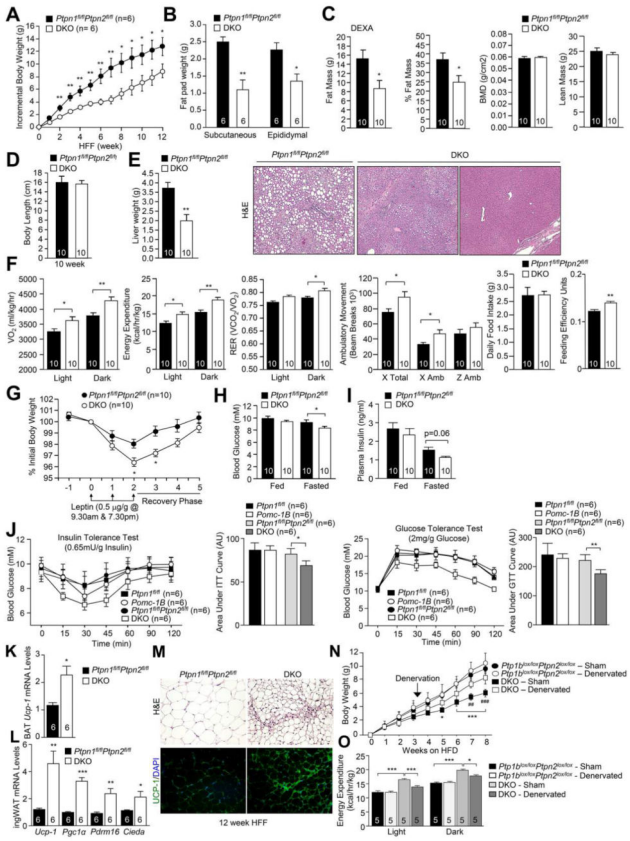

Figure 6. DKO mice are resistant to DIO

8 week-old *Ptpn1*$^{fl/fl}$*Ptpn2*$^{fl/fl}$ and DKO mice were HFF for 12 weeks and **a)** incremental body weight, **b)** fat pad weight, **c)** body composition, **d)** body length, **e**) liver weight and histology and **f)** oxygen consumption, energy expenditure, ambulatory activity, RER, food intake and feeding efficiency assessed. **g)** 12 week HFF mice were administered leptin and body weights monitored. Fed and fasted **h)** blood glucose and **i)** plasma insulin levels in 12 week HFF mice. **j)** Insulin and glucose tolerance tests in 12 week HFF mice. **k–m)** Browning gene expression, **m**) histology and immunohistochemistry in BAT or ingWAT from 12 week HFF mice. **n–o**) *Ptpn1*$^{fl/fl}$*Ptpn2*$^{fl/fl}$ and DKO mice were HFF and either sham-operated or bilaterally denervated after 3 weeks, high fat feeding continued for 5 weeks and **(n)** incremental body weights and **o)** energy expenditure measured. Results are means ± SEM for the indicated number of mice and are representative of 3 independent experiments; significance determined using a–b, f–g, i–j, n–o) two-way ANOVA. n) * corresponds to floxed v/s DKO sham operated; # DKO sham v/s DKO denervated.

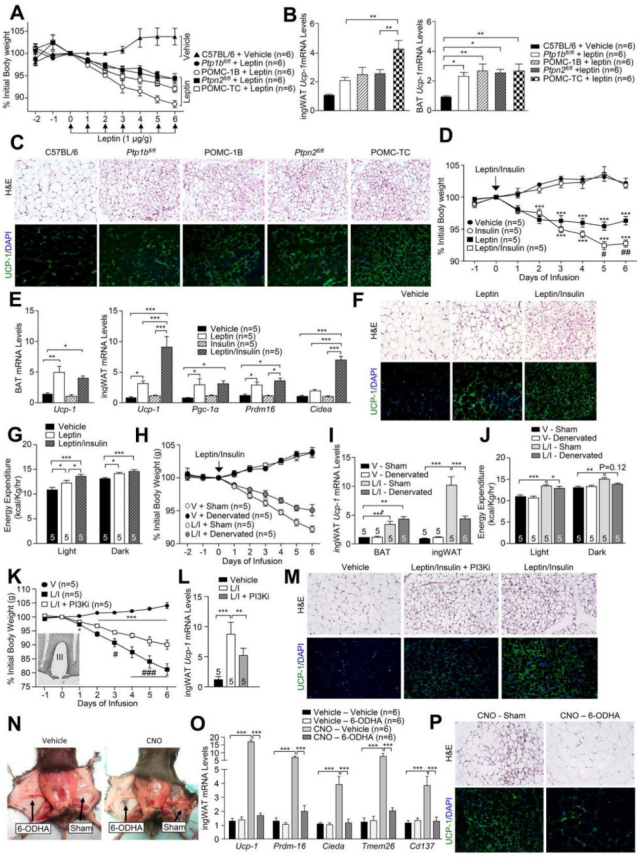

Figure 7. Leptin and insulin induce WAT browning

a–c) 8 week-old mice were administered leptin IP and **a**) daily body weights recorded, **b–c**) ingWAT and BAT extracted for **b**) analysis of *Ucp-1* gene expression, **c**) histology and immunohistochemistry; C57BL/6 mice were administered vehicle as a control. **d–g)** 8 week-old C57BL/6 mice were ICV infused vehicle, insulin (3 mU/day), leptin (4.8 μg/day) or insulin + leptin and **d**) body weights monitored, **e–f**) BAT and ingWAT extracted for **e**) gene expression analyses, **f**) histology and immunohistochemistry, and **g**) energy expenditure assessed. **h–j**) C57BL/6 mice were subjected to sham or ingWAT bilateral denervations (6-OHDA) and ICV infused with insulin + leptin and **h**) body weights, **i**) BAT and ingWAT *Ucp-1* expression and **j**) energy expenditure monitored. **k–m**) C57BL/6 mice were implanted with bilateral intra-ARC cannulas and infused with vehicle, insulin (3 mU/day) + leptin (4.8 μg/day) or insulin + leptin + PI3K inhibitor (PI3Ki; LY294002, 5 μg/day). **k**) Daily body weights were recorded (insert: intra-ARC cannula placement) and ingWAT extracted for **l**) analysis of *Ucp-1* gene expression, **m**) histology and UCP-1 immunohistochemistry. **n–p**) *Pomc*-Cre mice were bilaterally injected with rAAV-hSyn-DIO-hM3D(Gq)-mCherry into the ARC. Contralateral ingWAT depots were sham operated or denervated and the mice administered vehicle or CNO (1.5 mg/kg/day, IP) and ingWAT processed for **n**) *in situ* morphology, **o**) gene expression **p)** histology and immunohistochemistry. Data are means ± SEM and are representative of 3 independent experiments; significance determined using a, d, h, j) two-way ANOVA, or b, e, g, i, k, l, n, o) one-way ANOVA. d) * corresponds to leptin (L) or L/insulin (I) v/s vehicle (V); # L/I

versus L. h) * corresponds to L/I v/s V; # L/I sham v/s denervated. k) * corresponds to L/I, or L/I + PI3Ki v/s V; # L/I v/s L/I + PI3Ki.